Table 1. The ratios of the coefficients (b/a) in each of the three areas and motor neurons.

| | |
|---|---|
| MST neurons | acc. : vel. : pos. = 1 : 36.5 : -190.7 |
| DLPN neurons | acc. : vel. : pos. = 1 : 25.2 : -44.4 |
| Purkinje cells | acc. : vel. : pos. = 1 : 50.3 : -238.1 |
| motor neurons (from Keller's data) | acc. : vel. : pos. = 1 : 67.4 : 344.8 |

Table 2. Significance of each component in the reconstructed firing frequency

A Local Fitting using retinal slip

| MST | Number of Data Sets | | |
|---|---|---|---|
| | P < 0.005 | 0.005< P < 0.05 | 0.05< P |
| Acceleration component | 129 (73.7 %) | 0 ( 0.0 %) | 46 (26.3 %) |
| Velocity component | 133 (76.0 %) | 39 (22.3 %) | 3 ( 1.7 %) |
| Positional component | 53 (30.3 %) | 57 (32.6 %) | 65 (37.1 %) |

B

| DLPN | Number of Data Sets | | |
|---|---|---|---|
| | P < 0.005 | 0.005< P < 0.05 | 0.05< P |
| Acceleration component | 129 (80.6 %) | 0 ( 0.0 %) | 31 (19.4 %) |
| Velocity component | 125 (78.1 %) | 32 (20.0 %) | 3 ( 1.9 %) |
| Positional component | 34 (21.3 %) | 29 (18.1 %) | 97 (60.6 %) |

C

| VPFL | Number of Data Sets | | |
|---|---|---|---|
| | P < 0.005 | 0.005< P < 0.05 | 0.05< P |
| Acceleration component | 51 (51.0 %) | 0 ( 0.0 %) | 49 (49.0 %) |
| Velocity component | 83 (83.0 %) | 16 (16.0 %) | 1 ( 1.0 %) |
| Positional component | 22 (22.0 %) | 36 (36.0 %) | 42 (42.0 %) |

D Local Fitting using eye movement

| MST | Number of Data Sets | | |
|---|---|---|---|
| | P < 0.005 | 0.005< P < 0.05 | 0.05< P |
| Acceleration component | 165 (94.3 %) | 0 ( 0.0 %) | 10 ( 5.7 %) |
| Velocity component | 158 (90.3 %) | 6 ( 3.4 %) | 11 ( 6.3 %) |
| Positional component | 132 (75.4 %) | 12 ( 6.9 %) | 31 (17.7 %) |

E

| DLPN | Number of Data Sets | | |
|---|---|---|---|
| | P < 0.005 | 0.005< P < 0.05 | 0.05< P |
| Acceleration component | 157 (98.1 %) | 0 ( 0.0 %) | 3 ( 1.9 %) |
| Velocity component | 129 (80.6 %) | 11 ( 6.9 %) | 20 (12.5 %) |
| Positional component | 115 (71.9 %) | 15 ( 9.4 %) | 30 (18.7 %) |

F

| VPFL | Number of Data Sets | | |
|---|---|---|---|
| | P < 0.005 | 0.005< P < 0.05 | 0.05< P |
| Acceleration component | 95 (95.0 %) | 0 ( 0.0 %) | 5 ( 5.0 %) |
| Velocity component | 98 (98.0 %) | 2 ( 2.0 %) | 0 ( 0.0 %) |
| Positional component | 86 (86.0 %) | 2 ( 2.0 %) | 12 (12.0 %) |

The P values of the t-test indicate the significance probability of the null hypothesis that the coefficient of each component is zero. A-C: the tables of P values for MST (A), DLPN (B), and VPFL (C) by applying the model to retinal slip data. D-F: the tables of P values for MST (D), DLPN (E), and VPFL (F) by applying the model to eye movement. If the P value is small, model fitting is poor when that component is dropped.

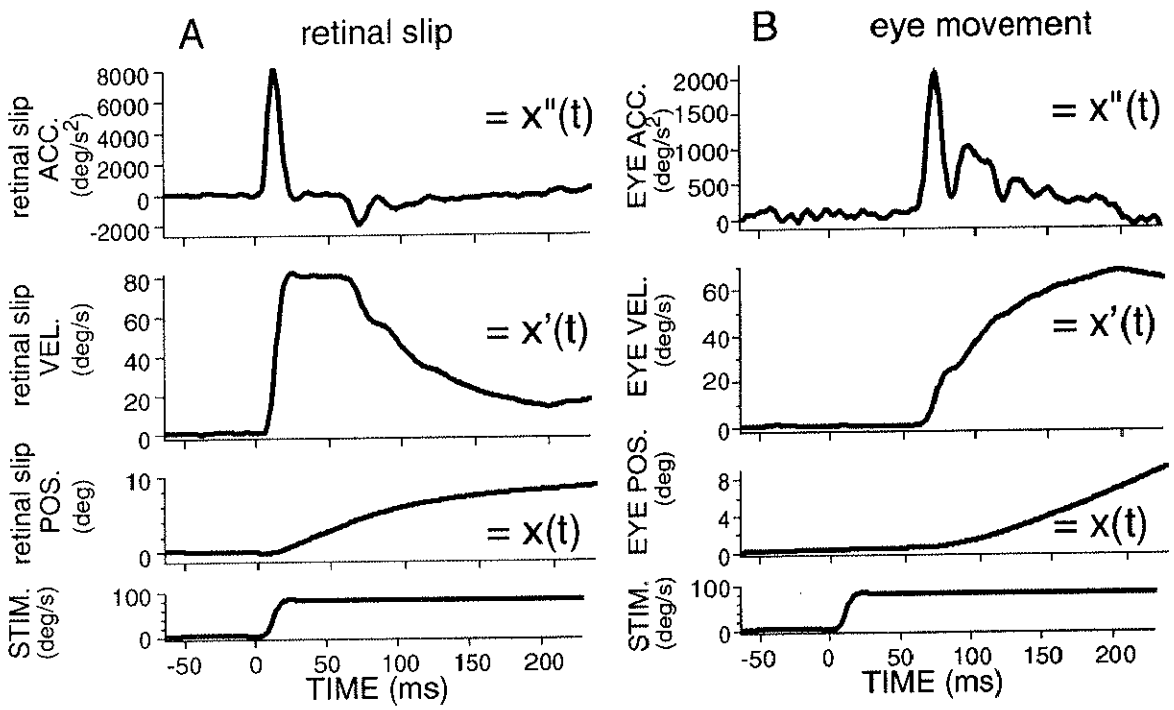


Figure 1. A: Retinal slip to downward ramps at 80 deg/s. The responses are aligned at stimulus onset. From top to bottom, ensemble averaged vertical retinal slip acceleration, velocity, and position, and averaged stimulus velocity profiles. Upward deflection in the figure indicates downward retinal slip or stimulus movements. B: Ocular following responses to downward ramps at 80 deg/s. The responses are aligned at stimulus onset. From top to bottom, ensemble averaged vertical eye acceleration, velocity, and position, and averaged stimulus velocity profiles. Upward deflection in the figure indicates downward eye or stimulus movements. All data were filtered with a Butterworth low-pass filter (cut-off, 50 Hz). STIM., stimulus velocity; POS., position; VEL, velocity; ACC., acceleration.

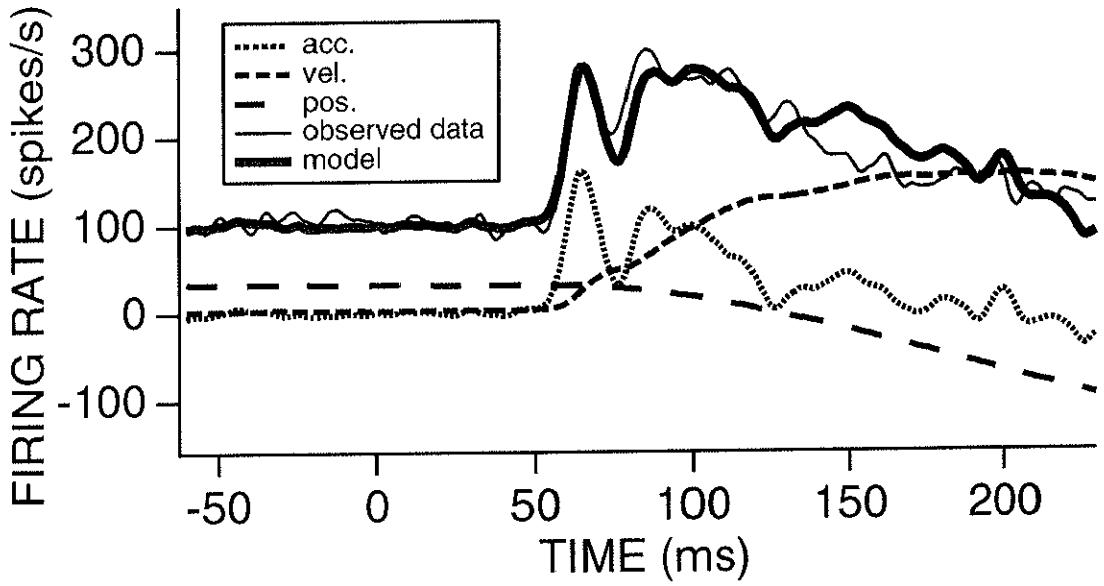


Figure 2. Reconstructed (thick line) and observed (thin line) simple spike firing pattern of a Purkinje cell in the ventral paraflocculus (VPFL) in response to preferred direction stimulus (downward) at 80 deg/s, and components of the reconstructed firing frequency ascribed to eye acceleration (dotted line), velocity (broken line), and position (dashed line). Estimated coefficients are a [0.134 (spikes/s)/(deg/s2)], b [2.13 (spikes/s)/(deg/s)], c [-13.2 (spikes/s)/deg], d [77.2 (spikes/s)], and a time lag component, delta (8 ms).

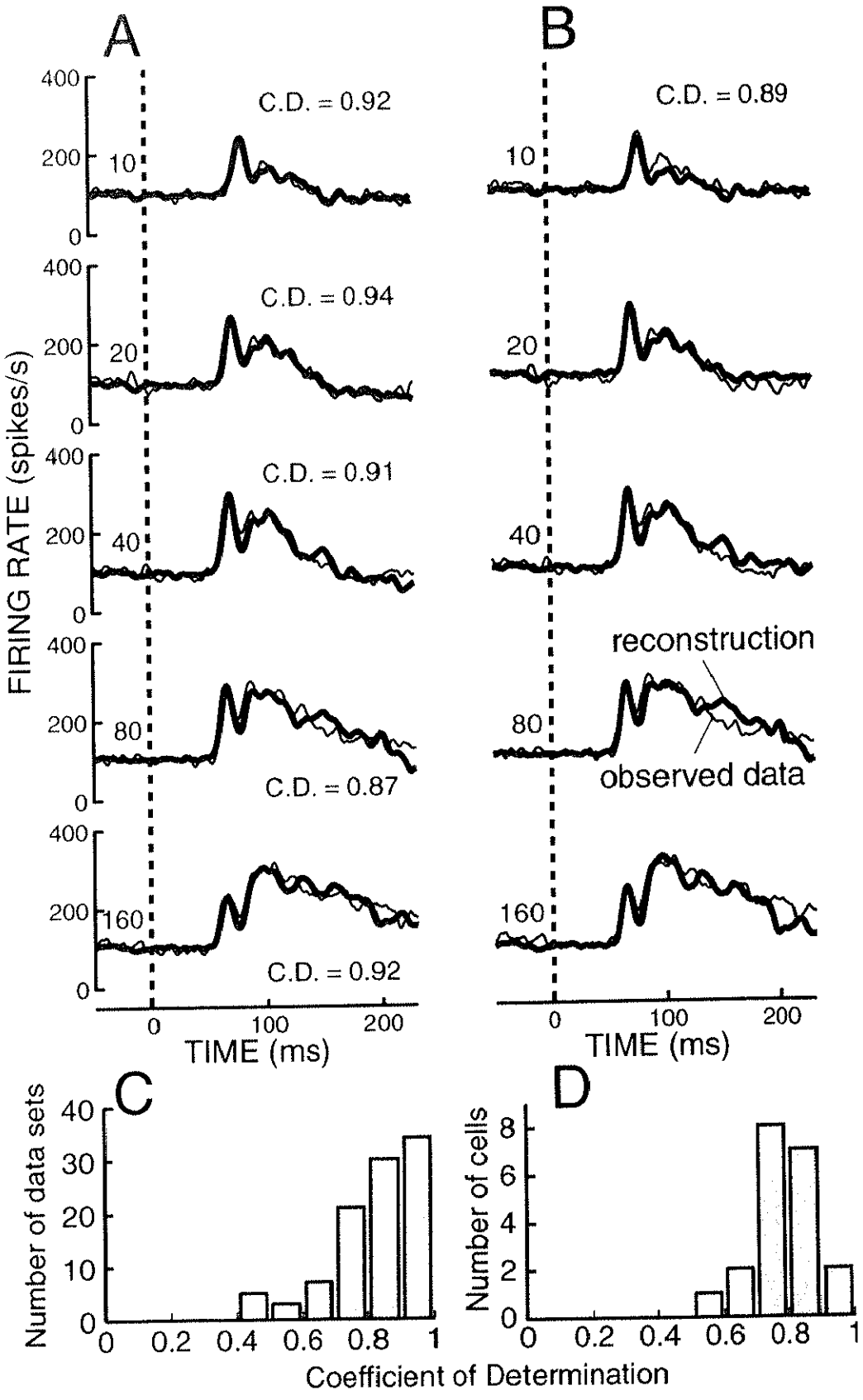


Figure 3. Reconstruction of the temporal patterns of the same P cell firing frequency as in Fig. 2 at the five stimulus velocities from eye movement. A: the model was separately applied to the firing pattern at each of the five stimulus speeds (Local Fitting). B: the model was applied to the firing patterns at all five stimulus speeds with a single set of the parameters (Global Fitting). Stimulus speed is indicated by the numbers at the left of the traces. Traces show the observed firing frequency profiles (thin line) and the reconstructed firing frequency profiles (thick line) from eye movement. Traces are aligned at the beginning of ramps (time = 0 ms). C and D: frequency histogram of the C.D.s for 100 data sets of the P cells (C) and for 20 P cells (D). Shaded areas: C.D. $\geqq$ 0.7

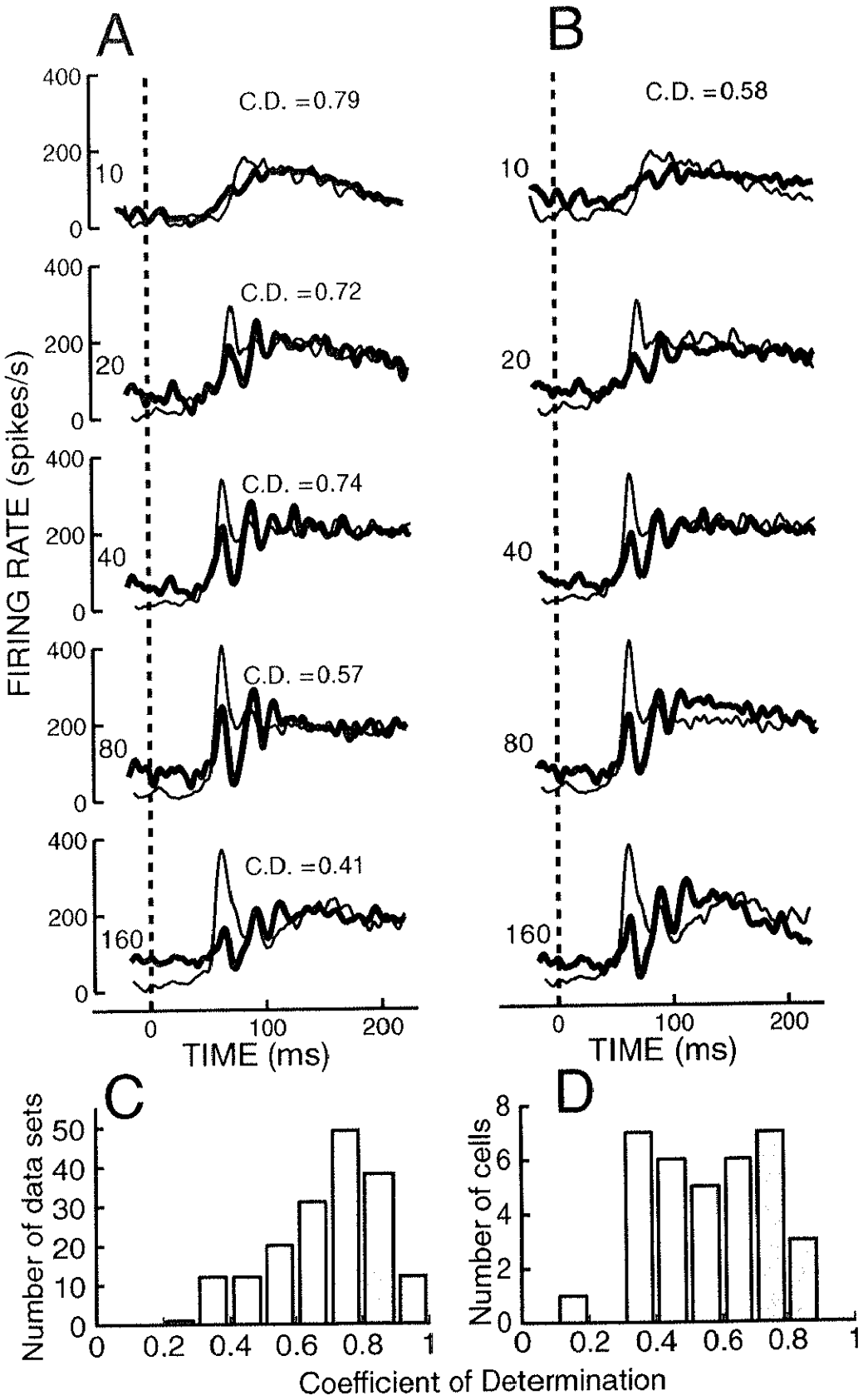


Figure 4. Reconstruction of the firing patterns of an MST neuron at the five stimulus velocities from eye movement. A: Local Fitting. B: Global Fitting. Stimulus speed is indicated by the numbers at the left of the traces. Traces are aligned at the beginning of ramps (time = 0 ms). C and D: frequency histogram of the C.D.s for 175 data sets of the MST neurons in (C) and for 35 MST neurons (D). Shaded areas: C.D. $\geqq$ 0.7

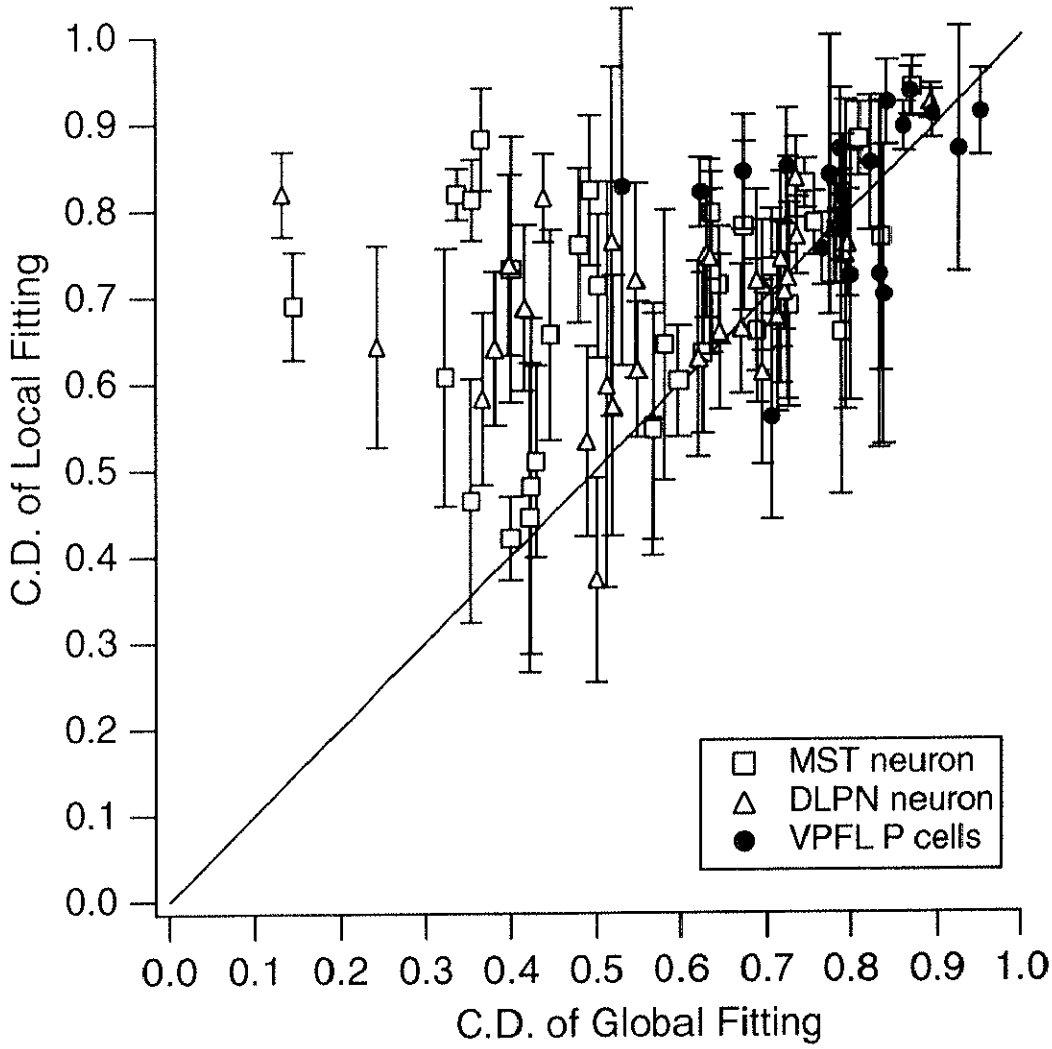


Figure 5. Summary of the reconstruction of the firing patterns in each area from eye movement using Local and Global Fitting. Each point indicates one of the MST neurons (open square), DLPN neurons (open triangle), and VPFL P cells (filled circle). The axis of abscissa represents the C.D.s of Global Fitting and the axis of ordinate represents the C.D.s of Local Fitting. For Global Fitting, one C.D. was calculated for each neuron. For Local Fitting, since the model was applied separately to the responses at each of the five speeds, five C.D.s were calculated for each neuron; the mean and the standard deviation are plotted.

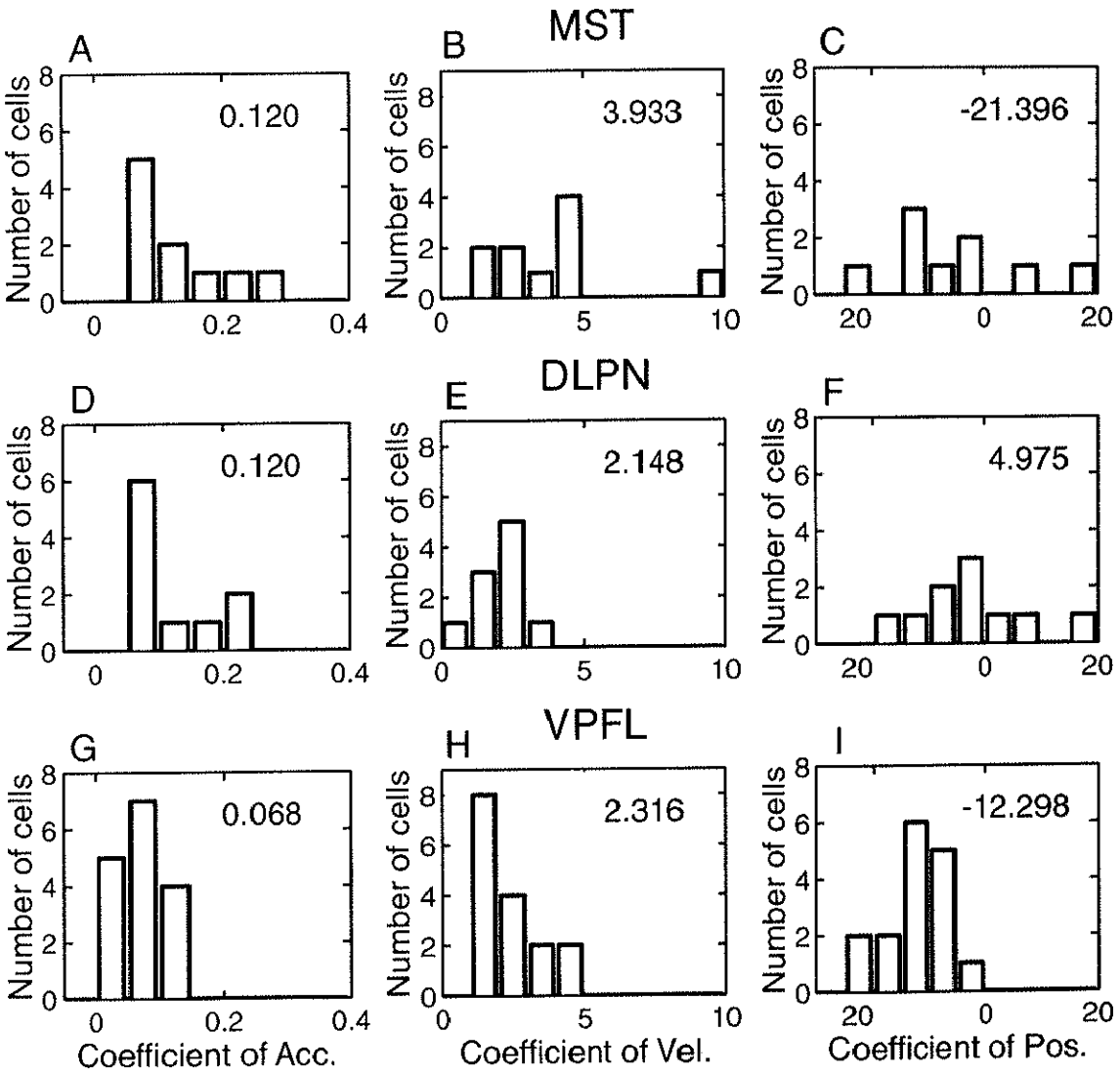


Figure 6. Comparison of the distributions of estimated coefficients [acceleration coefficients ( A, D, and G), velocity coefficients (B, E, and H), and position coefficients (C, F, and I)] using Global Fitting from eye movement in each of the three areas. A-C: the distributions of each coefficient for 10 MST neurons. D-F: the distributions of each coefficient for 10 DLPN neurons. G-I; the distributions of each coefficient for 16 P cells. The mean values of each coefficient of the three areas are indicated by the numbers at the middle of the middle column. Note: In C and F, there are some stray data points (2/10 MST and 1/10 DLPN) with values beyond the range of the graph.

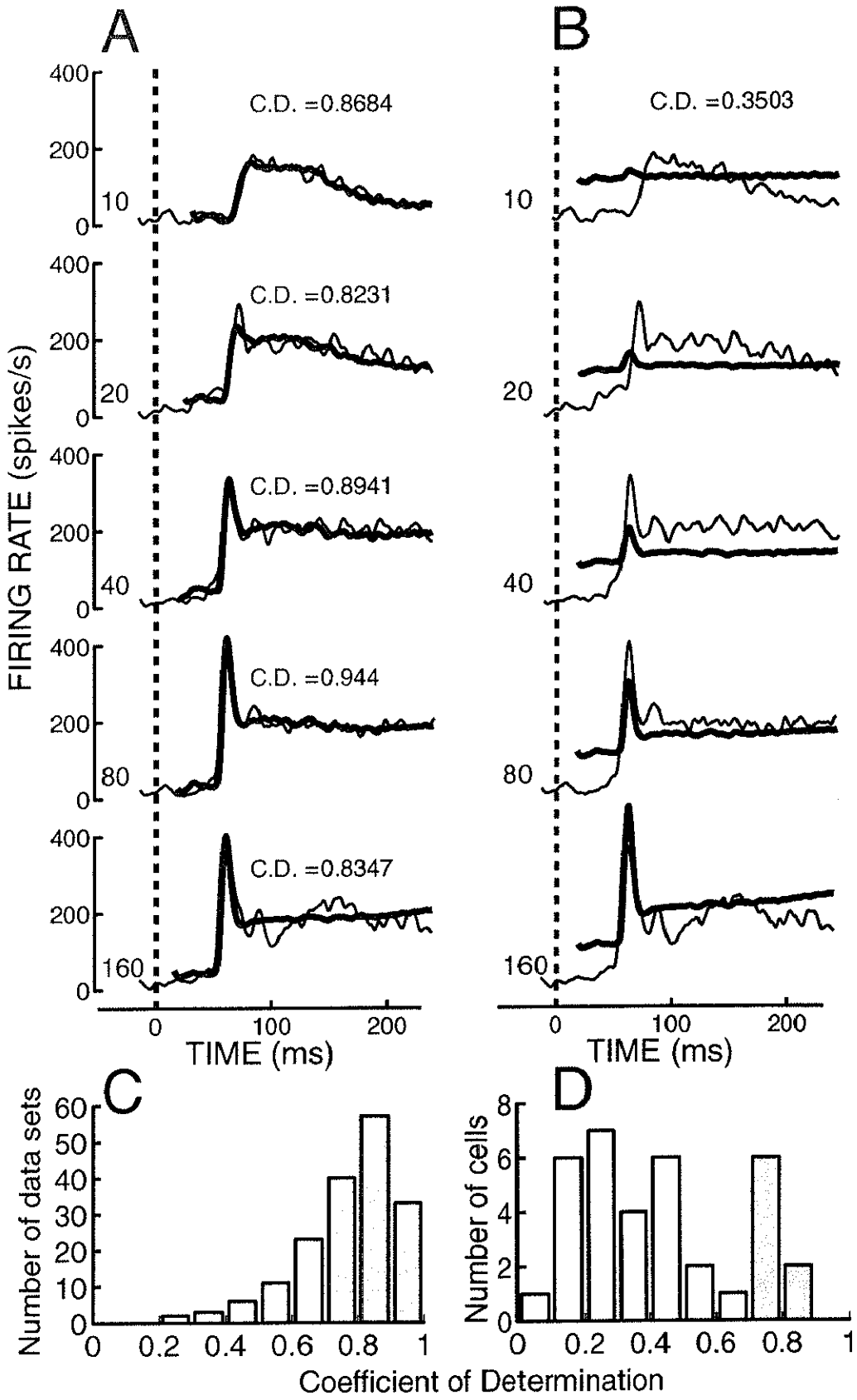


Figure 7. Reconstruction of the firing patterns of the same MST neuron as in Fig. 4 at the five stimulus velocities from retinal slip data. A: Local Fitting. B: Global Fitting. Stimulus speed is indicated by the numbers at the left of the traces. Traces are aligned at the beginning of ramps (time = 0 ms). C and D: frequency histogram of the C.D.s for 175 data sets of the MST neurons (C) and for 35 MST neurons in (D). Shaded areas: C.D. $\geqq 0.7$

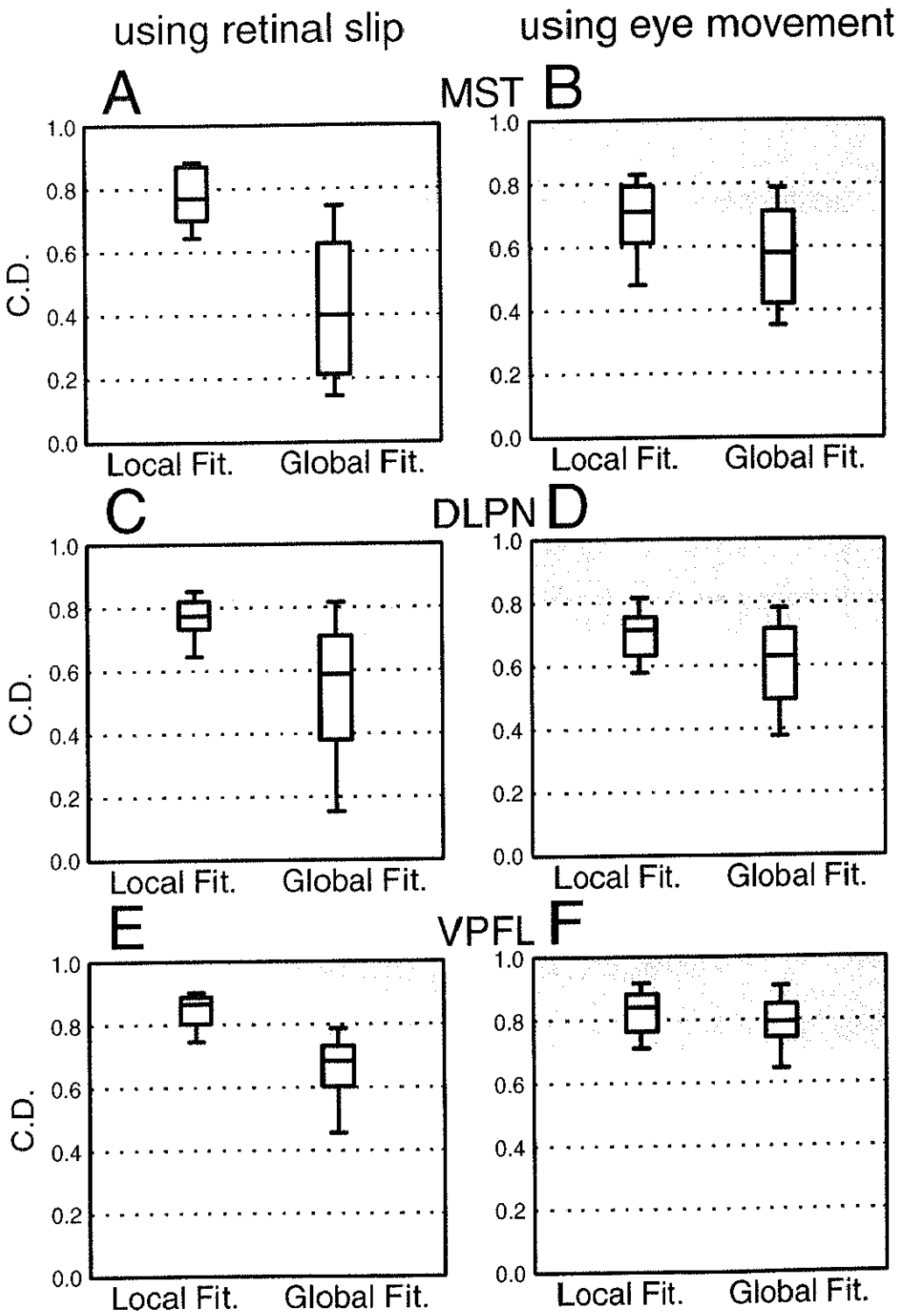


Figure 8. Summary of the linear-regression analysis for the cells in the MST (A and B), DLPN (C and D), and VPFL (E and F) from eye movement or retinal slip using Local (left) or Global Fitting (right). A, C, and E: Distribution of C.D.s of the cells in each of the three areas using retinal slip data. B, D, and F: Distribution of C.D.s of the cells in each of the three areas using eye movement. Each box plot shows the 10, 25, 50, 75, and 90 percentiles of distribution.

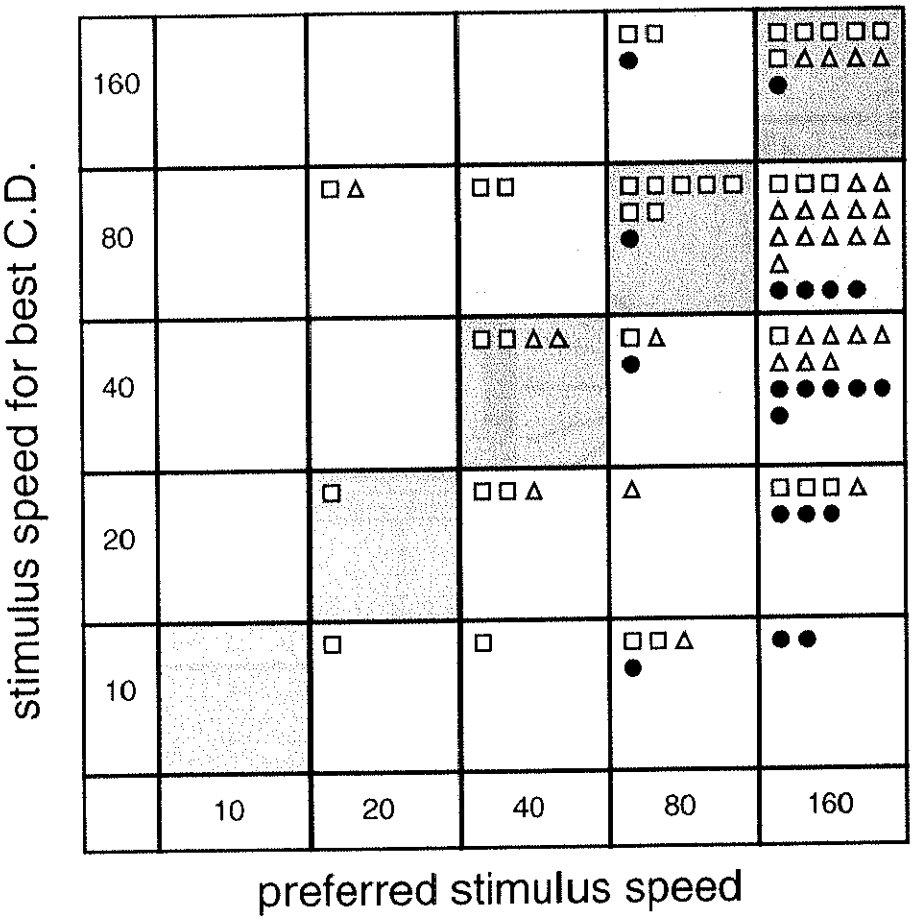


Figure 9. Relationship between optimal speeds for the neural responses and speeds for the best C.D. of reconstruction. The open squares, triangles, and filled circles represent individual MST neurons, DLPN neurons, and VPFL P cells, respectively, and are plotted in the square of the optimal speed for the neural responses (axis s of abscissa) and in the square of the speed for the best C.D. of reconstruction (axis of ordinate).

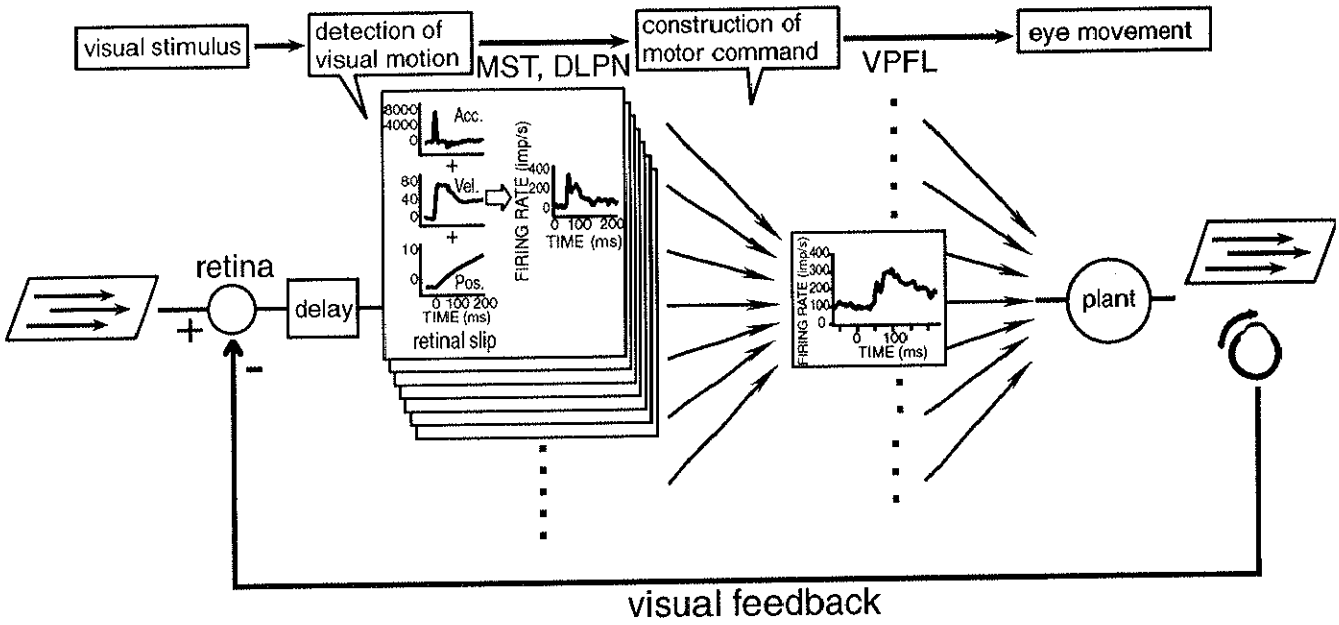


Figure 10. Schematic representation of signal flow in the brain during generation of ocular following.